

Probability distributions of the induced electric field of the solar wind

B. Breech, W. H. Matthaeus, L. J. Milano, and C. W. Smith

Bartol Research Institute, University of Delaware, Newark, Delaware, USA

Received 10 June 2002; revised 20 November 2002; accepted 29 January 2003; published 11 April 2003.

[1] The low-frequency induced electric field in the near-Earth interplanetary medium is investigated observationally. These electric field fluctuations are associated with magnetohydrodynamic-scale fluctuations of the magnetic field and plasma velocity. Results of the study, based upon hourly samples with variations computed relative to 4-day means, indicate that the electric field distribution is roughly exponential. More specifically, the electric field distribution is very nearly the one that is obtained from a quasi-normal turbulence model [Milano *et al.*, 2002]. These results may be useful for particle scattering, acceleration, and turbulence. *INDEX TERMS*: 2164 Interplanetary Physics: Solar wind plasma; 2149 Interplanetary Physics: MHD waves and turbulence; 2752 Magnetospheric Physics: MHD waves and instabilities; 2712 Magnetospheric Physics: Electric fields (2411); *KEYWORDS*: solar wind, electric field, pdf, MHD turbulence

Citation: Breech, B., W. H. Matthaeus, L. J. Milano, and C. W. Smith, Probability distributions of the induced electric field of the solar wind, *J. Geophys. Res.*, 108(A4), 1153, doi:10.1029/2002JA009529, 2003.

1. Introduction

[2] Interplanetary magnetohydrodynamic (MHD) fluctuations [Jokipii, 1971; Goldstein *et al.*, 1995; Tu and Marsch, 1995] have numerous connections to solar wind and cosmic ray physics [Matthaeus *et al.*, 1999; Bieber *et al.*, 1994; Droege, 2000] and to turbulence theory [Matthaeus and Goldstein, 1982]. Most widely studied have been characteristics of magnetic field fluctuations and (proton) velocity and density fluctuations at timescales from several days down to spacecraft instrumental resolution. The typical characteristics are powerlaw spectra of magnetic and velocity fields at observed scales ranging from several hours to several seconds. This is often associated with an MHD direct cascade of energy in the incompressible flow. Cross correlation of the velocity and magnetic field, associated with the ideally conserved MHD cross helicity, signifies a dominant sense of outward propagation in the inner heliosphere with a systematic tendency towards zero cross helicity and balanced implied propagation direction with increasing heliocentric distance [Roberts *et al.*, 1987a, 1987b]. The evolution of the MHD fluctuation spectrum, the heating of the solar wind, and the scattering of energetic particles all involve to some degree the generation of electric field fluctuations which have been largely unexplored.

[3] In the present paper we present some basic observational characteristics of the MHD electric field \mathbf{E} which has received relatively less attention, and in particular the induced electric field (see below) which is expected to be the dominant contribution throughout most of space. We compute the frequency of occurrence of values of the fluctuating induced electric field, viewing these as estimates

of the probability distribution functions (PDFs) of the same quantities. These are the fundamental probabilistic measures defining the one point statistical ensemble of the fluctuating induced electric field. Related statistical measures such as the kurtosis (see equation (12) below) are also computed. We find that the statistics of induced electric field fluctuations are well described by the assumption of Gaussian statistics of the fluctuating velocity and the fluctuating magnetic field. Thus, the observed distributions of induced electric field are seen to be consistent with a recent theory [Milano *et al.*, 2002] based upon the quasi-Gaussian or quasi-normal assumption.

[4] The dynamical importance of the electric field is embodied in the magnetic field \mathbf{B} induction equation,

$$\frac{\partial \mathbf{B}}{\partial t} = -c \nabla \times \mathbf{E} \quad (1)$$

where c is the speed of light. In magnetohydrodynamic (MHD) models of plasma dynamics, the electric field is usually expressed by a constitutive relation, a generalized Ohm's Law,

$$\mathbf{E} = -\frac{\mathbf{V}}{c} \times \mathbf{B} + \frac{\mathbf{j}}{\sigma} + \mathbf{E}_c \quad (2)$$

where σ is the conductivity, $(4\pi/c) \mathbf{j} = \nabla \times \mathbf{B}$ is the electric current, and \mathbf{V} is the velocity field. Kinetic contributions to the electric field, such as Hall and electron pressure effects, are included in \mathbf{E}_c . The magnetic induction equation is then written as

$$\partial_t \mathbf{B} = \nabla \times (\mathbf{V} \times \mathbf{B} - c \mathbf{E}_c) + \eta \nabla^2 \mathbf{B}, \quad (3)$$

with $\eta = c^2/(4\pi\sigma)$.

[5] We are principally concerned with characterization of the electric fields associated with turbulent fluctuations, that is the induced electric field produced by the fluctuations of the velocity and magnetic fields. We defer to a later time an attempt to answer the question as to whether the values of the induced electric field are comparable to the values of the total electric field, and what relationship might exist between the statistics of the induced electric field and the statistics of the total electric field. For the present we will neglect the collisionless electric field \mathbf{E}_c , and note that in space plasmas such as the solar wind the collisional η is typically small. In turbulence research, it has become customary to employ Alfvén speed units by the transformation $\mathbf{B} \rightarrow \mathbf{B}/\sqrt{4\pi\rho}$ where ρ is the local mean proton number density [Matthaeus and Goldstein, 1982]. \mathbf{V} and \mathbf{B} are then measured in km/sec. In this way we focus on the inductive electric field $\mathbf{E} = -\mathbf{V} \times \mathbf{B}$, which we now subject to a turbulence decomposition.

[6] In the usual way, the fields \mathbf{V} and \mathbf{B} are separated into mean and fluctuating parts according to

$$\mathbf{V} = \mathbf{V}_0 + \mathbf{v}, \quad \mathbf{B} = \mathbf{B}_0 + \mathbf{b}, \quad (4)$$

where $\mathbf{V}_0 = \langle \mathbf{V} \rangle$, $\mathbf{B}_0 = \langle \mathbf{B} \rangle$ and the $\langle \rangle$ operator denotes an appropriate ensemble average. Note that, by definition,

$$\langle \mathbf{v} \rangle = 0 = \langle \mathbf{b} \rangle. \quad (5)$$

In the context of homogeneous turbulence [e.g., Batchelor, 1970], ensemble averaged quantities are translation invariant, i.e., they do not depend upon position. In an inhomogeneous medium such as the solar wind, ensemble averages can still be defined but are expected to vary in space and time. If the medium is weakly inhomogeneous in an appropriate sense [see, e.g., Monin and Yaglom, 1971, 1975; Matthaeus and Goldstein, 1982] the statistics can be viewed as locally homogeneous. This is the approach taken, for example, in mean field electrodynamics [Krause and Rädler, 1980] and in engineering turbulence models such as "K- ϵ " models [Bradshaw et al., 1981]. We define the fluctuating component of the electric field as

$$\delta\mathbf{e} \equiv -\mathbf{v} \times \mathbf{b} + \langle \mathbf{v} \times \mathbf{b} \rangle. \quad (6)$$

We also define

$$\mathbf{E}_0 \equiv \langle \mathbf{E} \rangle = -\mathbf{V}_0 \times \mathbf{B}_0 - \langle \mathbf{v} \times \mathbf{b} \rangle. \quad (7)$$

[7] In mean field electrodynamics and other applications it is convenient to divide the equation of motion for the magnetic field (3) into mean and fluctuating parts, from which we can see the several effects of induced electric field. Neglecting kinetic and dissipative terms, one finds

$$\partial_t \mathbf{B}_0 = -\nabla \times \mathbf{E}_0 \quad (8)$$

and

$$\partial_t \mathbf{b} = -\nabla \times \delta\mathbf{e} + \nabla \times (\mathbf{v} \times \mathbf{B}_0 + \mathbf{V}_0 \times \mathbf{b}). \quad (9)$$

It is the quantity $\delta\mathbf{e}$ that we are mainly concerned with here, which drives magnetic turbulence through equation (9),

although the "mean EMF" of the fluctuations $\langle \mathbf{v} \times \mathbf{b} \rangle$ is of considerable interest as well in dynamo theory [Krause and Rädler, 1980; Moffatt, 1978] because of its role in the dynamics of the large-scale field in equation (8).

[8] The fluctuating induced electric field of the solar wind is a topic that has received very little attention in the literature. Marsch and Tu [1992] presented a spectral analysis of the electric field for one day of Helios data. Recently, le Roux et al. [2001] provided a model for pickup ion acceleration that relies upon the one-point statistics of the fluctuating electric field. Lacking evidence to the contrary, they assumed a Gaussian distribution for the electric field fluctuations. Below we will show that there is a different distribution of electric field fluctuations realized in the interplanetary medium, and it is one that can be understood by a simple theory; namely, that the components of velocity and magnetic field are approximately Gaussian. However, the induced electric field is highly non-Gaussian.

2. Observations

[9] We examine data from the NSSDC Omnitape data set [King and Papitashvili, 1994], which consists of 1 hour magnetic and velocity field averages from over 30 years. The data is broken down into 4 day intervals, which is much longer than a typical correlation time in the solar wind, and much shorter than the solar rotation period (about 28 days). Furthermore, the mean fields can be determined reasonably well over 4 days and there is a good chance that the interval will not have sections consisting of different statistical properties. Earlier studies [Matthaeus and Goldstein, 1982; Padhye et al, 2001] have shown that averaging intervals on the order of four days give reasonable and stable results for many solar wind fluctuation properties of interest.

[10] Spacecraft data commonly has gaps of missing data, which can cause problems when computing statistics. Furthermore, in the Omnitape set, at some times there is a valid measurement of \mathbf{B} , but no corresponding measurement of \mathbf{V} . Since we are investigating the electric field, these points have to be rejected. If more than 25% of the data is missing or rejected in a given interval, we choose to discard that interval. This leads to rejecting nearly 80% of the available intervals, leaving about 30,000 points for analysis. That number is further shortened by avoiding sector crossings of the satellites. This drops the number of data points down to about 5,500. (The analysis was also repeated by increasing the tolerance of missing data to 35%. We will remark more about this case later on.)

[11] Once the data is broken up into intervals, we convert \mathbf{B} into Alfvén speed units, $\mathbf{B} \rightarrow \mathbf{B}/\sqrt{4\pi\rho}$ where ρ is the four-day measured mean proton number density. This change allows more direct comparisons of the magnitudes of the two fields. Throughout the remainder of the paper, both velocity and magnetic field will have units of km/sec and the electric field will be in km^2/sec^2 . The means of \mathbf{B} and \mathbf{V} are calculated for each interval. Following that, coordinates are transformed into mean field coordinates, which is a natural system where the correlation function is axisymmetric [Belcher and Davis, 1971]. For the rest of the paper, the "z" direction corresponds to the direction of the mean magnetic field, with "x" and "y" directions being perpendicular to "z" in a right handed coordinate system.

[12] We define two averaging operators for this paper. The first is

$$\langle x \rangle_I = \frac{1}{N(I)} \sum_{i=1}^{N(I)} x_i \quad (10)$$

which is the typical averaging of data for a single interval with $N(I)$ points in it. The second averaging operator is

$$\langle f \rangle = \sum_{I=1}^{N_{int}} \frac{N(I)}{N_{tot}} \langle f \rangle_I \quad (11)$$

which is a weighted average of the quantity f calculated across N_{int} intervals. N_{tot} is the total number of data points available.

[13] We begin by characterizing the distribution of the electric field by calculating the (central) kurtosis, which we compare with similar computations for velocity and magnetic field fluctuations. The kurtosis, K , is defined as

$$K \equiv \frac{\langle x^4 \rangle}{\langle x^2 \rangle^2} \quad \text{with} \quad \langle x \rangle = 0. \quad (12)$$

The kurtosis can be viewed as a property of the population or as a property of the distribution function (see Appendix A). In the latter perspective it provides a sense of how far the distribution is from Gaussian. Equation (12) can be used to show that a Gaussian distribution has a kurtosis of exactly 3. Distributions with lower values of K are more concentrated near low values than a Gaussian. Distributions with higher values of K are flatter, often exhibiting distinctive ‘‘tails,’’ corresponding to elevated probability of values with large magnitudes.

[14] A useful way to estimate kurtosis is to calculate K for each data interval and then average over all intervals. For the present analysis results computed in this way are listed in the ‘‘Average. Intervals’’ column of Table 1. The components of \mathbf{b} are close to Gaussian, with numbers similar to those reported by *Padhye et al.* [2001]. The components of \mathbf{v} also come out close to Gaussian. For the magnetic field components, near-Gaussianity is well established [*Whang, 1977; Padhye et al., 2001*] and it has been previously reported for velocity increments with long time lags [*Sorriso-Valvo et al., 1999; Marsch and Tu, 1994*].

[15] Another method for calculating the kurtosis is by population statistics. Here, the kurtosis is calculated over the entire data, instead of just over an interval (in all cases the four-day mean values are used to extract \mathbf{v} and \mathbf{b}). Table 1 shows that the kurtosis of the components of \mathbf{v} and \mathbf{b} increase, on average, by 55%. This suggests that the distribution functions for \mathbf{v} and \mathbf{b} are approximately Gaussians of varying widths, a possibility also explored by *Padhye et al.* [2001]. The variability of the widths of the distributions is not a small effect - the four-day variances of the components of \mathbf{v} and \mathbf{b} vary from a low of 8.5 to a high of 112. These results point towards a definition of an ensemble in which the component variances are used as similarity variables.

[16] It is desirable to examine the data over the entire 30 day span, particularly to compare against theoretical results

Table 1. Summary of the Kurtosis Values, From Averaging the Value Computed for Each Interval, and From the Entire Population, With Four Day Means Removed

Component	Average Intervals	Population
v_x	2.88 ± 0.30	4.11
v_y	4.40 ± 0.62	6.57
v_z	2.67 ± 0.11	4.07
b_x	2.98 ± 0.16	3.81
b_y	3.77 ± 0.19	6.96
b_z	3.43 ± 0.19	5.18

for the electric field. Since the data is composed of intervals with varying local values of the variances (sigma values), lumping them together would result in a skewed distribution. For example, adding two Gaussian distributions with different sigma values gives a non-Gaussian distribution. Therefore, we normalize the data in order to look at the functional form of the electric field distribution for the entire data set.

[17] We rescale the component data in each interval by the field’s standard deviation,

$$f_{\alpha,j}^I \rightarrow \tilde{f}_{\alpha,j}^I \equiv \frac{f_{\alpha,j}^I}{\sigma(f_{\alpha}^I)} \quad (13)$$

where f stands for either \mathbf{v} , \mathbf{b} , or $\delta\mathbf{e}$, α refers to the Cartesian component, j is the j th element in the interval, I is the particular interval of data considered, and σ is the standard deviation of a data interval computed in the sense of equation (10). This normalization has been used by others, such as *Sorriso-Valvo et al.* [1999]. It should be stressed that this normalization is done for each field separately so that $\delta\mathbf{e}$ is calculated from the raw data and then normalized, rather than calculated from the normalized \mathbf{v} and \mathbf{b} components.

[18] The drawback of this normalization is that information about rotational symmetry and possible variance anisotropy will be lost, as the variance of each component, as calculated from equation (11), will be unity. In light of this, other normalizations were considered, such as normalizing by the magnetic energy, the flow energy, or the total magnetic-plus-flow energy; but (13) has the nice property that the kurtosis of the population is conserved, that is,

$$\begin{aligned} K(\tilde{f}_{\alpha}) &= \frac{1}{N} \sum_{I=1}^{N_{int}} \sum_{j=1}^{N(I)} \left(\tilde{f}_{\alpha,j}^I \right)^4 \\ &= \sum_{I=1}^{N_{int}} \frac{N(I)}{N} \left[\frac{1}{N(I)} \sum_{j=1}^{N(I)} \left(\frac{f_{\alpha,j}^I}{\sigma(f_{\alpha}^I)} \right)^4 \right] = \langle K(f_{\alpha}) \rangle, \end{aligned} \quad (14)$$

where the mean operator is defined in equation (11). In addition, we remark that the present normalization scheme brings the computed kurtosis values of \mathbf{v} and \mathbf{b} in an overall sense closer to the Gaussian value than do the other normalization procedures that we implemented.

[19] Table 2 shows the result of the normalization on the kurtosis values of the components of \mathbf{v} and \mathbf{b} . It is clear that the raw (not normalized) population statistics obscured the underlying Gaussian nature of the distributions, whereas normalizing by equation (13) reveals this feature more clearly.

Table 2. Kurtosis Values of \mathbf{v} and \mathbf{b} After Normalization by the Individual Four-Day Component Variance

Component	x	y	z
\mathbf{b}	2.97	3.80	3.42
\mathbf{v}	2.85	4.48	2.62

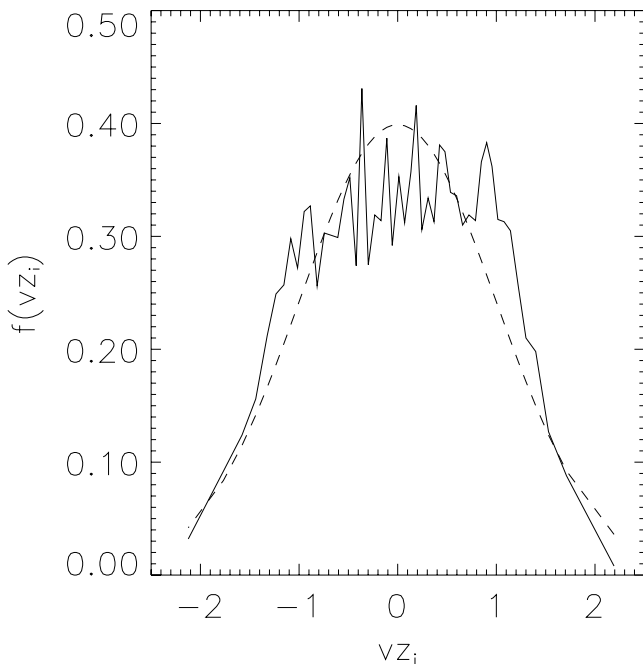
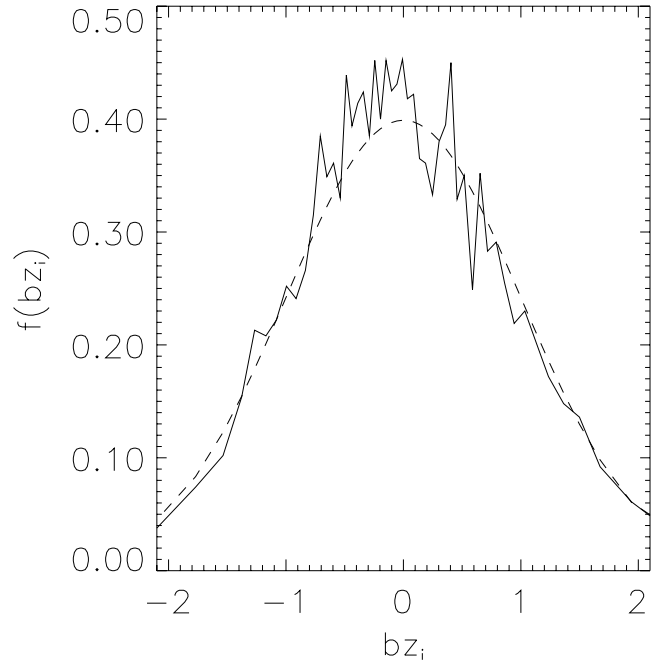
[20] We now proceed, using the component normalization scheme, to characterize the probability distribution functions (PDFs) of the components of the fluctuating electric field, which we estimate by calculating the frequency of occurrence of the normalized quantities from four-day intervals over the entire 30 year data set. To begin we recall the properties of the PDFs of the velocity and magnetic field fluctuations [see, e.g., *Padhye et al., 2001*, and references therein]. Figures 1 and 2 show the PDFs for the z component of the velocity and magnetic fields, respectively. For illustration purposes, the dashed line shows a Gaussian distribution using the same half-width calculated from the data. The components of \mathbf{v} and \mathbf{b} typically are not very far from Gaussian distributions.

3. Comparison to Theoretical Results

[21] In previous work [*Milano et al., 2002*], we considered the PDF of a variable of the form

$$s = x_1x_2 - x_3x_4 \quad (15)$$

representing a component of the induced electric field of the fluctuations $\mathbf{e} = -\mathbf{v} \times \mathbf{b}$. In view of the observed properties of the distribution of components of \mathbf{v} and \mathbf{b} , the Gaussian approximation is applied to x_1, x_2, x_3 and x_4 . In the simplest

**Figure 1.** PDF for z -component of the velocity field. The dashed curve is a Gaussian distribution with the same σ value.**Figure 2.** PDF for z -component of the magnetic field. The dashed curve is a Gaussian distribution with the same σ value.

case, in which these variables can be assumed statistically independent Gaussian variables, the PDF for s is shown to be $f(s) \approx e^{-|s|}$ (see equation (20) below). This case is consistent with a system with no mean induced electric field and zero cross helicity. To model more realistic physical scenarios, we considered correlations between the Gaussian variables x_i . In particular, suppose there is a substantial cross helicity, so that corresponding components of \mathbf{v} and \mathbf{b} are correlated. Then an electric field component s will involve correlations between x_1 and x_4 and between x_2 and x_3 . Suppose also that the mean electric field is zero, so $\langle x_1x_4 \rangle = \langle x_2x_3 \rangle$. For this case, *Milano et al. [2002]* have shown that the PDF for s is given by

$$f(s) = \frac{1}{\sqrt{2}\sigma_s} \text{gexp} \left(\rho_{14}, \rho_{23}, -\frac{\sqrt{2}}{\sigma_s} |s| \right), \quad (16)$$

$$\rho_{ij} \equiv \frac{\langle x_i x_j \rangle}{\sigma_i \sigma_j}, \quad (17)$$

where ρ_{ij} provides measure of the cross correlation. Here gexp is a “generalized exponential” defined by

$$\text{gexp}(\rho_1, \rho_2, z) \equiv \frac{\sqrt{1 - \rho_1 \rho_2}}{2\pi} \int_0^{2\pi} \exp \left(\frac{\Theta_1}{\Theta_2} \sqrt{\frac{1 - \rho_1 \rho_2}{1 - \rho_1^2}} z \right) \frac{d\theta}{\Theta_1 \Theta_2}, \quad (18)$$

$$\Theta_i \equiv \sqrt{1 - \rho_i \sin(2\theta)}. \quad (19)$$

Table 3. Cross Correlations Associated With Computing Components of Induced Electric Field

Component		ρ_{14}	ρ_{23}
e_x	$x_1 = v_z, x_2 = b_y$	-0.025 ± 0.037	-0.30 ± 0.033
	$x_3 = v_y, x_4 = b_z$		
e_y	$x_1 = v_z, x_2 = b_z$	-0.12 ± 0.034	-0.025 ± 0.037
	$x_3 = v_z, x_4 = b_x$		
e_z	$x_1 = v_x, x_2 = b_y$	-0.12 ± 0.034	-0.30 ± 0.033
	$x_3 = v_y, x_4 = b_x$		

Note that in the absence of cross helicity (e.g. $\rho_{14} = \rho_{23}$), then g_{exp} becomes just an exponential function and equation (16) becomes

$$f(s) = \frac{1}{\sqrt{2}\sigma_s} \exp\left(-\frac{\sqrt{2}}{\sigma_s}|s|\right), \quad (20)$$

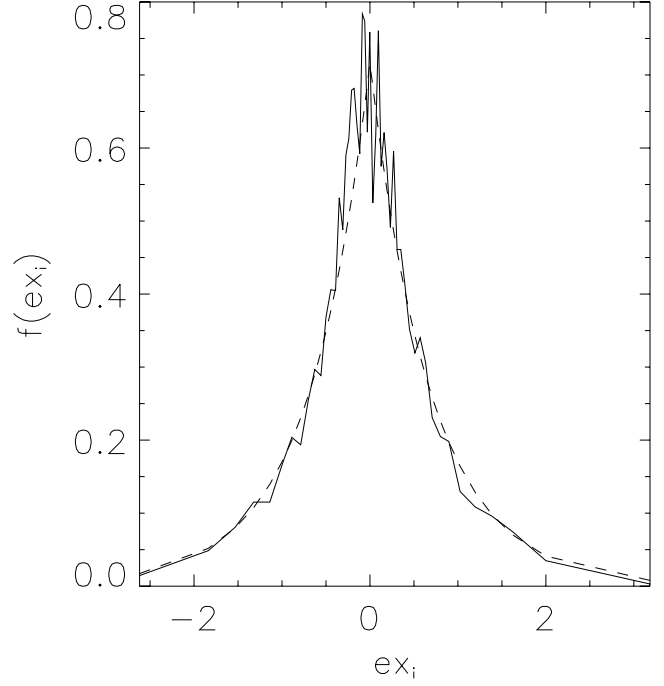
a simple exponential distribution function.

[22] Solar wind turbulence is often characterized by the presence of ‘‘Alfvénic fluctuations’’ having a sign of cross helicity associated with a preponderance of outward traveling waves. Since this is a familiar property both at low heliographic latitudes [Belcher and Davis, 1971] and in the high-latitude fast wind [Bavassano et al., 2000], departures of the electric field distribution from the pure exponential form are a possibility. The generalized exponential form would be expected to be relevant when the selected ensemble of solar wind fluctuations has a significant non-zero cross helicity.

[23] It should be noted that the above distributions, equations (16) and (20) are the expected distributions for any component of $-\mathbf{v} \times \mathbf{b}$ provided that \mathbf{v} and \mathbf{b} have Gaussian distributions and $\langle \mathbf{v} \times \mathbf{b} \rangle = 0$ (see Appendix B for a brief discussion of the effects on \mathbf{e} when \mathbf{v} and \mathbf{b} depart from Gaussian). This last condition is approximately satisfied by our data, as follows. We find that the mean of the components of $\langle \mathbf{v} \times \mathbf{b} \rangle$ are 11, -3.8 , and 18.8 (km^2/sec^2), and the r.m.s. values for these components are 195, 386 and 288 (km^2/sec^2). A typical value of δe is 1930 km^2/sec^2 (see section 4), so we conclude that the means are relatively small. As a consequence, $\delta e \approx \mathbf{e} = -\mathbf{v} \times \mathbf{b}$. To simplify the notation, we will use \mathbf{e} instead of δe from now on.

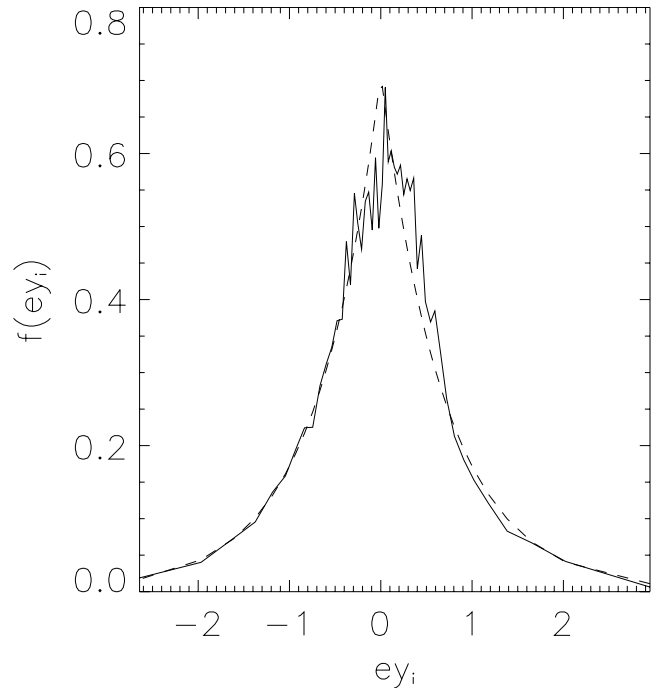
[24] Table 3 shows values of the cross correlation ρ of the components of \mathbf{e} , computed from the Omnitape data intervals. The values are small. Figures 3, 4, and 5 show the PDFs for each component of the electric field. The solid line is the PDF calculated from the data, while the dashed line is equation (16), which includes contributions from the computed cross correlations. The PDFs were calculated using $n = 50$ bins. (See Appendix A) The number of bins is large enough that the kurtosis values stop dropping dramatically, but short enough that the kurtosis does not become meaningless. Since the correlations are weak, the PDFs for the components of \mathbf{e} are very close to the simple exponential, equation (20). The maximum difference for any of the graphs from the simple exponential is 0.01.

[25] The value of the kurtosis predicted by equation (16) lies between 6 and 9, where 6 is obtained in the limit in which the PDF tends to an exponential (i.e. equation (20)). The kurtosis, calculated by population statistics, for the components shown in the Figures are 7.9, 6.0, and 7.2 for the x, y and z components respectively. The kurtosis values indicate that the distributions are more peaked than a typical

**Figure 3.** Distribution function of the x-component of induced electric field computed from normalized data. The dashed curve is equation (16).

Gaussian distribution, which has a kurtosis of 3. This is also evident from the figures.

[26] The above analysis was repeated by increasing the tolerance of missing data from 25% to 35%. This results in increasing the total number of available points from 5,500

**Figure 4.** Distribution function of the y-component of induced electric field computed from normalized data. The dashed curve is equation (16).

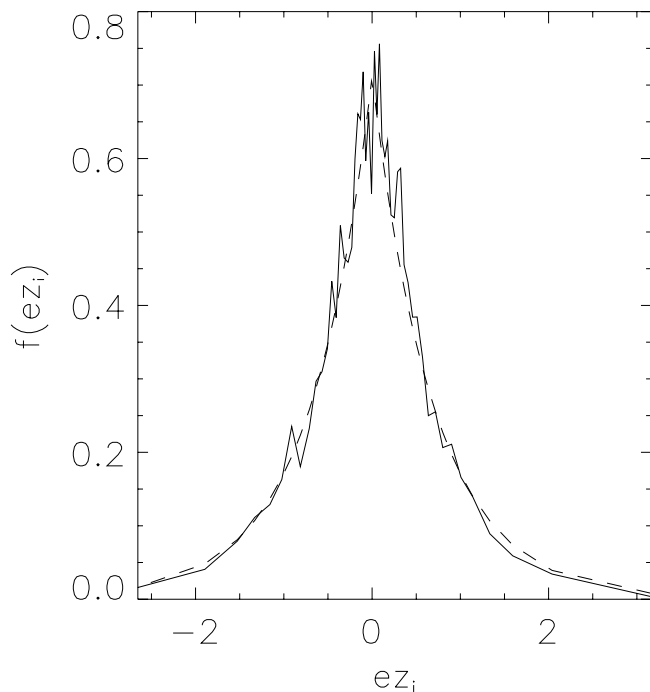


Figure 5. Distribution function of the z-component of induced electric field computed from normalized data. The dashed curve is equation (16).

to 12,000, and increasing the reported kurtosis values of the x and y components of the electric field by 0.3, or roughly 5%. The z component, which corresponds to the direction of the mean \mathbf{B} field, showed no increase. From this, we conclude that our results are stable. However, it should be noted that the means of \mathbf{V} and \mathbf{B} on each interval are less well defined with the higher tolerance because of the increase in missing data, so we choose the 25% tolerance as a compromise value.

4. Strength of the Induced Electric Field

[27] The normalization methods of the previous section provide insight into the underlying degree of Gaussianity of the turbulence, but, in so doing, explicitly avoided the issue of mean values of the dynamic fields. As discussed in the Introduction, the mean strength of the induced electric field is, in general, an important consideration in characterizing the structure and dynamics of MHD turbulence. More specifically, the interplanetary medium in the inner heliosphere (and to some degree at 1 AU) has been described as “Alfvénic” [e.g., *Belcher and Davis*, 1971] in that frequently observed correlations between velocity and magnetic fluctuations are diagnostic of “outward traveling” waves. For such a state, one expects $\mathbf{v} \approx \mathbf{b}$ or $\mathbf{v} \approx -\mathbf{b}$ depending upon whether the mean magnetic field \mathbf{B}_0 is inward directed, or outward directed, respectively. Despite the frequent occurrence of correlations of this type, the fluctuations are rarely if ever purely outwards [*Bavassano et al.*, 1982; *Tu and Marsch*, 1995; *Matthaeus and Goldstein*, 1982] and, moreover, it is well known that the degree of this “Alfvénicity” is observed to decrease with increasing heliocentric distance [*Roberts et al.*, 1987b]. In view of the

elementary vector identity $|\mathbf{v}|^2|\mathbf{b}|^2 = (\mathbf{v} \cdot \mathbf{b})^2 + |\mathbf{v} \times \mathbf{b}|^2$, it follows that whenever the directional Alfvénic correlation is not exactly obtained, there must be an induced electric field. This is true, of course, provided there is energy density in both magnetic and velocity fields. The spatially varying part of this electric field enters directly into the fluctuation dynamics through equation (9). Thus it would be a mistake to conclude that the appearance of partial or approximate Alfvénic correlation indicates a lack of turbulent dynamics. Indeed the strength of the induced electric field can be taken as one measure of the strength of turbulent couplings in a magnetoplasma such as the solar wind.

[28] The simplest measure of the strength of turbulent induced electric fields is the mean value

$$\delta e = \langle (\mathbf{v} \times \mathbf{b} - \langle \mathbf{v} \times \mathbf{b} \rangle)^2 \rangle^{1/2}. \quad (21)$$

From the analysis presented above, this value is found to be $\delta e = 1930 \text{ (km/sec)}^2 \approx 1.98 \times 10^{-4} \text{ V/m}$ assuming a typical proton density of 5 protons/cc). A heuristic comparison may be made with the computed root mean square velocity, $\delta v = 67 \text{ km/sec}$, and root mean square magnetic field $\delta b = 36 \text{ km/sec}$. One sees that δe is about 80% of the product $\delta v \delta b$, indicating a strong turbulent induced electric field.

[29] As another measure we employ a formula for Gaussian isotropic turbulence given by *Oughton et al.* [1997]. Their equation (34) expresses the mean square turbulent electric field δe^2 in terms of the magnetic and flow energies as well as the cross helicity. It should be emphasized that this relationship is not precise for anisotropic turbulence, but provides nevertheless an interesting comparison. The Oughton et al. formula states that the maximum δe^2 , for zero cross helicity, is $\delta e_{\{G\}}^2 = (2/3)\delta v^2\delta b^2$; using δv^2 and δb^2 from our analysis gives $\delta e_{\{G\}}^2 \approx 3.8 \times 10^6 \text{ (km/sec)}^2$. This is to be compared with the observationally computed value of $\delta e^2 = 3.7 \times 10^6 \text{ (km/sec)}^2$.

5. Conclusions

[30] We have presented a study of the one-point statistics of the induced electric field associated with low-frequency solar wind fluctuations. We employed Omnitape data at 1 AU and our conclusions can be summarized as follows. The fluctuating induced electric field $\mathbf{e} = -\mathbf{v} \times \mathbf{b}$ is described by an approximately exponential distribution with kurtosis values between 6 and 9, consistent with predictions derived for nearly Gaussian distributions of the fluctuating \mathbf{v} and \mathbf{b} fields. This theoretical result is well-confirmed in the present observational analysis. This means that the “natural” state of induced electric field fluctuations is to be somewhat more peaked at low values than would be a Gaussian (such as the magnetic field or velocity fields individually), and also to have an exponential tail. The net effect is a distribution that would typically be interpreted as less space-filling than a Gaussian. Second we examined the typical strengths of the turbulent induced electric field. This is a quantity that is, in a very basic sense, the driver of the dynamics of magnetic turbulence; see equation (9). It is a measure of the turbulence that is complementary to the notion of Alfvénic turbulence. Higher Alfvénicity is associated with reduced induced electric field - in the limit of purely unidirectionally propagating fluctuations the equa-

tions of motion are linearized, the turbulent induced electric field vanishes, and there is no turbulence (in the incompressible limit; see *Moffatt* [1978]). Quantitatively we found typical strengths of turbulent induced electric field of ≈ 1100 (km/sec)² in Alfvén speed units, corresponding to roughly 80–90% of the value expected for zero cross helicity non-Alfvénic fluctuations. In this sense the turbulence at 1 hour scales at 1 AU should be expected to be very active.

[31] We should emphasize that all of the present analysis is carried out using 1 hour velocity and magnetic field data at 1 AU, employing four-day intervals to compute mean values. This corresponds, roughly, to the lower wave number end of the inertial range, since the correlation scale at 1AU typically corresponds to the ~ 10 hour scale in the spacecraft frame [*Matthaeus et al.*, 1999]. There is of course the possibility that the statistical properties of the electric field will be different in other ranges of space and time-scales, and we defer such studies to future efforts along these lines. Induced electric field properties may also vary with heliocentric distance. As the Alfvénic correlations decrease with increasing heliocentric distance [*Roberts et al.*, 1987b], the relative strength of induced electric field is expected to increase.

[32] The one point statistics we described here will have implications for some models of particle acceleration [e.g., *Le Roux et al.*, 2001] but more general formulations of electric field effects on particle scattering and acceleration [*LeRoux et al.*, 2002] require knowledge of the two point statistics (correlation functions and spectra) that are also beyond the scope of the present study. Finally we remark that future studies of this type may also examine possible implications for dynamo theory, although it has been remarked previously [*Lantz et al.*, 1983; *Marsch and Tu*, 1992] that local mean induced electric fields that would produce dynamo action through equation (8) are observed to be rather weak.

Appendix A: Computation of Probability Distribution Functions

[33] We take all N points of data, order them sequentially from minimum to maximum values, and partition them into n bins, with each bin containing m contiguous elements from the sorted list. N , n and m are clearly related by the simple relation $N = nm$.

[34] The probability distribution function can then be defined as

$$f(b_i) = \frac{1}{N} \frac{m}{\Delta b_i}. \quad (\text{A1})$$

Δb_i is the width of the bin, and b_i is the arithmetic mean of all the points in the bin.

[35] We can now proceed to calculate moments of the distribution function. The kurtosis is defined (assuming $\langle x \rangle = 0$) as,

$$K(x) = \frac{\int x^4 f(x) dx}{\left(\int x^2 f(x) dx \right)^2}. \quad (\text{A2})$$

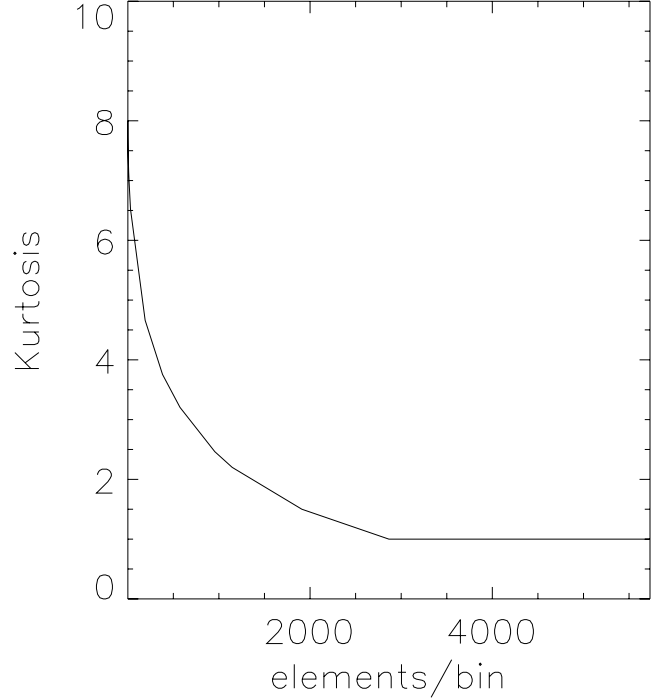


Figure 6. Kurtosis of the normalized x-component of induced electric field, computed from the estimated PDF, vs. the number of elements per bin used in describing the PDF. The “center” of the each bin is the arithmetic mean of the points in the bin.

Since our data is not continuous, we approximate the integrals in equation (A2) as discrete sums,

$$K(x) = \frac{\sum_{i=1}^n b_i^4 f(b_i) \Delta b_i}{\left(\sum_{i=1}^n b_i^2 f(b_i) \Delta b_i \right)^2}. \quad (\text{A3})$$

The other moments are defined similarly. Using equation (A3), we can now obtain the kurtosis in yet another way. We now wish to examine differences between this method and population statistics.

[36] The choice of n , or m , has a drastic effect upon the characteristics of the PDF, and any value calculated from it. As a limiting case, if we choose $m = 1$, then each bin has one point, and the kurtosis becomes identical to the kurtosis calculated from population statistics. In the opposite limit, if we pick $m = N$, then there is only one bin, and the kurtosis becomes unity. An example of this behavior is seen in Figure 6 for the x component of the normalized electric field. The changes in the kurtosis values are expected because of the sensitivity of the kurtosis of a random variable to its large values. The x^4 term in equation (A2) gives more emphasis to the large values. The act of binning data in order to use equation (A1) effectively “hides” some of the larger values since the center of each bin is the arithmetic mean of all the points in the bin. One could try to replace the arithmetic mean of the data points with simply the largest value in the bin. This changes Figure 6 a little bit as the kurtosis value actually increases for small values of m , but then starts to decrease again as m increases, as can be

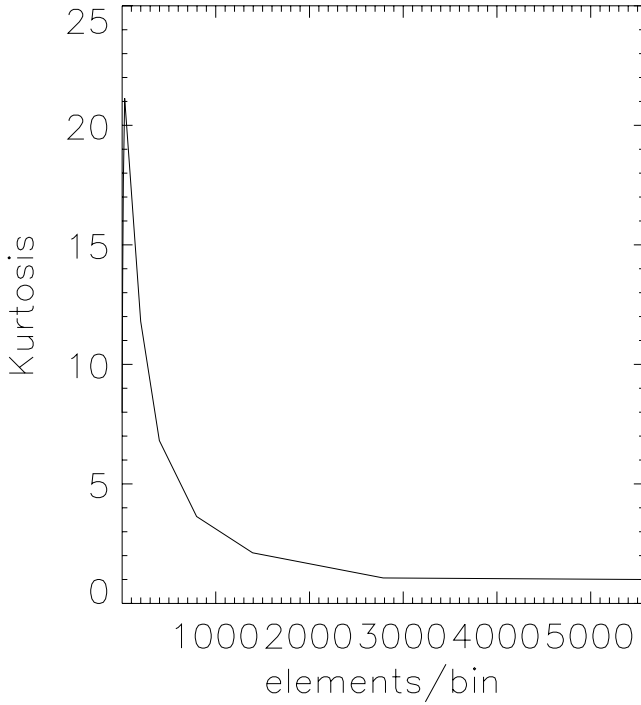


Figure 7. Kurtosis of the normalized x-component of induced electric field, computed from the estimated PDF, vs. the number of elements per bin used in describing the PDF. The “center” of each bin is taken to be the largest value in that bin.

seen in Figure 7. Finally, it should be noted that this behavior affects all moments, except the zeroth and first moments, which remain unchanged.

[37] The usefulness of creating a PDF as in equation (A1) lies in being able to build a more intuitive grasp of the information available from the statistical population. In light of the above discussion, however, calculating information directly from the PDF should be avoided. Instead, use the population statistics.

Appendix B: Gaussian Alfvénic Variables

[38] It is far from trivial to quantify a priori the effects of the departure from Gaussianity in the velocity and magnetic fields, in the statistics of the induced electric field. One may think that a small departure from Gaussianity in \mathbf{v} and \mathbf{b} would reflect itself in a small departure of the Gaussian prediction [Milano *et al.*, 2002] for $\mathbf{e} \equiv -\mathbf{v} \times \mathbf{b}$. However, this is not necessarily the case. As an example, we consider an expansion where both the fluctuating velocity and magnetic fields are expanded in a Gaussian component plus a small perturbation:

$$\mathbf{v} = \mathbf{v}_G + \epsilon \mathbf{v}_p, \quad (\text{B1})$$

$$\mathbf{b} = \mathbf{b}_G + \epsilon \mathbf{b}_p, \quad (\text{B2})$$

where by Alfvénicity we mean $\mathbf{v}_G = \pm \mathbf{b}_G$. We further assume that the perturbed components are statistically independent from the Gaussian components, and that all

components have zero mean. It turns out that as ϵ tends to zero, the statistics of \mathbf{v} and \mathbf{b} tend to be Gaussian in a trivial way. For example, the Kurtosis for each of these variables converges very rapidly to the Gaussian value of 3:

$$K(b_i) = 3 + \epsilon^4 \frac{\langle b_{pi}^2 \rangle^2}{\langle b_{Gi}^2 \rangle^2} (K(b_{pi}) - 3) + O(\epsilon^6). \quad (\text{B3})$$

[39] However, the statistics of the induced electric field are not dominated by the Gaussian components. This is because of the geometrical constraint imposed by the Alfvénicity, that implies:

$$\mathbf{e} = -\epsilon \mathbf{v}_p \times \mathbf{b}_G - \epsilon \mathbf{v}_G \times \mathbf{b}_p - \epsilon^2 \mathbf{v}_p \times \mathbf{b}_p \quad (\text{B4})$$

The statistics of the induced electric are therefore determined (to the lowest order in ϵ) in equal footing by the statistics of both the Gaussian and the perturbed components (note the symmetry in equation (B4) when the $O(\epsilon^2)$ term is neglected). To illustrate the idea, we note that in the simple case of which $\mathbf{v}_p = (v_{px}, 0, 0)$ and $\mathbf{b}_p = 0$, the kurtosis of the z component of the induced electric field is given by:

$$K(e_z) = K(b_{Gy})K(v_{px}) = 3K(v_{px}). \quad (\text{B5})$$

Clearly, $K(e_z)$ can get arbitrarily large, independently of the value of ϵ . In particular, in the limit $\epsilon \rightarrow 0$, the statistics of \mathbf{v} and \mathbf{b} tend to Gaussianity very fast, while the statistics for \mathbf{e} may remain extremely far from the Gaussian prediction.

[40] **Acknowledgments.** This research is supported in part by NSF under grant ATM-0105254, and by NASA under grants NAG5-8134, NAG5-6570 and NAG5-10911 at the University of Delaware.

[41] Shadia Rifai Habbal thanks Gordon D. Holman and Vincenzo Carbone for their assistance in evaluating this paper.

References

- Batchelor, G. K., *The Theory of Homogeneous Turbulence*, Cambridge Univ. Press, New York, 1970.
- Bavassano, B., M. Dobrowolny, F. Mariani, and N. F. Ness, Radial evolution of power spectra of interplanetary Alfvénic turbulence, *J. Geophys. Res.*, *87*, 3617, 1982.
- Bavassano, B., E. Pietropaolo, and R. Bruno, On the evolution of outward and inward Alfvénic fluctuations in the polar wind, *J. Geophys. Res.*, *105*, 15,959, 2000.
- Belcher, J. W., and L. Davis Jr., Large-amplitude Alfvén waves in the interplanetary medium, *2*, *J. Geophys. Res.*, *76*, 3534, 1971.
- Bieber, J. W., W. H. Matthaeus, C. W. Smith, W. Wanner, M. Kallenrode, and G. Wibberenz, Proton and electron mean free paths: The Palmer consensus revisited, *Astrophys. J.*, *420*, 294, 1994.
- Bradshaw, P., T. Cebeci, and J. Whitelaw, *Engineering Calculation Methods for Turbulent Flow*, Academic, San Diego, Calif., 1981.
- Droge, W., Particle scattering by magnetic fields, *Space Sci. Rev.*, *93*, 121, 2000.
- Goldstein, M. L., D. A. Roberts, and W. H. Matthaeus, Magnetohydrodynamic turbulence in the solar wind, *Annu. Rev. Astron. Astrophys.*, *33*, 283, 1995.
- Jokipii, J. R., Propagation of cosmic rays in the solar wind, *Rev. Geophys.*, *9*, 27, 1971.
- King, J., and N. Papitashvili, *Interplanetary Medium Data Book - Supplement 5, 1988-1993, Rep. NSSDC/WDC-A-R and S 94-08*, NASA, Greenbelt, Md., 1994.
- Krause, F., and K.-H. Rädler, *Mean-Field Magnetohydrodynamics and Dynamo Theory*, Akademie, Berlin, 1980.
- Lantz, S., W. H. Matthaeus, and M. L. Goldstein, Preliminary determination of the “alpha-effect dynamo” parameter in the solar wind, *Eos Trans. AGU*, *64*, 822, 1983.

- le Roux, J., W. Matthaeus, and G. Zank, Pickup ion acceleration by turbulent electric fields in the slow solar wind, *Geophys. Res. Lett.*, *28*, 3831, 2001.
- le Roux, J. A., G. P. Zank, L. J. Milano, and W. H. Matthaeus, A quasi-linear kinetic theory for charged-particle transport in two-dimensional turbulence, *Astrophys. J.*, *567*, L155–L158, 2002.
- Marsch, E., and C. Y. Tu, Electric field fluctuations and possible dynamo effects in the solar wind, in *Proceedings of Solar Wind 7, COSPAR Colloq. Ser.*, vol. 3, edited by E. Marsch and R. Schwenn, p. 505, Pergamon, Tarrytown, N.Y., 1992.
- Marsch, E., and C. Y. Tu, Non-Gaussian probability distributions of solar wind fluctuations, *Ann. Geophys.*, *12*, 1127, 1994.
- Matthaeus, W. H., and M. L. Goldstein, Measurement of the rugged invariants of magnetohydrodynamic turbulence in the solar wind, *J. Geophys. Res.*, *87*, 6011, 1982.
- Matthaeus, W. H., G. P. Zank, C. W. Smith, and S. Oughton, Turbulence, spatial transport, and heating of the solar wind, *Phys. Rev. Lett.*, *82*, 3444, 1999.
- Milano, L. J., W. H. Matthaeus, B. Breech, and C. W. Smith, One-point statistics of the induced electric field in quasi-normal magnetofluid turbulence, *Phys. Rev. E*, *65*, 026310-1–026310-8, 2002.
- Moffatt, H. K., *Magnetic Field Generation in Electrically Conducting Fluids*, Cambridge Univ. Press, New York, 1978.
- Monin, A., and A. Yaglom, *Statistical Fluid Mechanics*, vol. 1, MIT Press, Cambridge, Mass., 1971.
- Monin, A., and A. Yaglom, *Statistical Fluid Mechanics*, vol. 2, MIT Press, Cambridge, Mass., 1975.
- Oughton, S., K.-H. Rädler, and W. H. Matthaeus, General second-rank correlation tensors for homogeneous magnetohydrodynamic turbulence, *Phys. Rev. E*, *56*, 2875, 1997.
- Padhye, N., C. W. Smith, and W. H. Matthaeus, Distribution of magnetic field components in the solar wind plasma, *J. Geophys. Res.*, *106*, 18,635, 2001.
- Roberts, D. A., L. W. Klein, M. L. Goldstein, and W. H. Matthaeus, The nature and evolution of magnetohydrodynamic fluctuations in the solar wind: Voyager observations, *J. Geophys. Res.*, *92*, 11,021, 1987a.
- Roberts, D. A., M. L. Goldstein, L. W. Klein, and W. H. Matthaeus, Origin and evolution of fluctuations in the solar wind: Helios observations and Helios-Voyager comparisons, *J. Geophys. Res.*, *92*, 12,023, 1987b.
- Sorriso-Valvo, L., V. Carbone, P. Veltri, G. Consolini, and R. Bruno, Intermittency in the solar wind turbulence through probability distribution functions of fluctuations, *Geophys. Res. Lett.*, *26*, 1801, 1999.
- Tu, C.-Y., and E. Marsch, MHD structures, waves and turbulence in the solar wind, *Space Sci. Rev.*, *73*, 1, 1995.
- Whang, Y., Probability distribution functions of microscale magnetic fluctuations during quiet conditions, *Sol. Phys.*, *53*, 507–517, 1977.

B. Breech, W. H. Matthaeus, L. J. Milano, and C. W. Smith, Bartol Research Institute, University of Delaware, Newark, Delaware 19716, USA. (breech@cis.udel.edu)